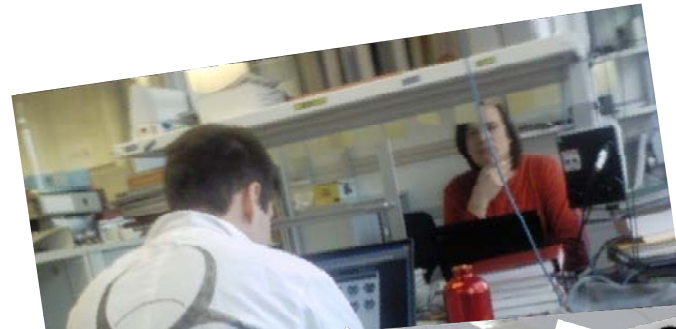




Thermodynamic Modeling of Materials for Solid Oxide Fuel Cells

Erwin Povoden-Karadeniz





Solid Oxide Fuel Cells (SOFC): Chemical energy → Electrical energy

Chromium “poisoning” of planar SOFC

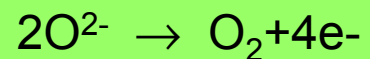
Calphad (**C**alculation of **p**hase **d**iagrams) modeling

Thermodynamic La-Sr-Mn-Cr oxide database

Applications: SOFC cathodes poisoned by chromium

Principles of planar SOFC

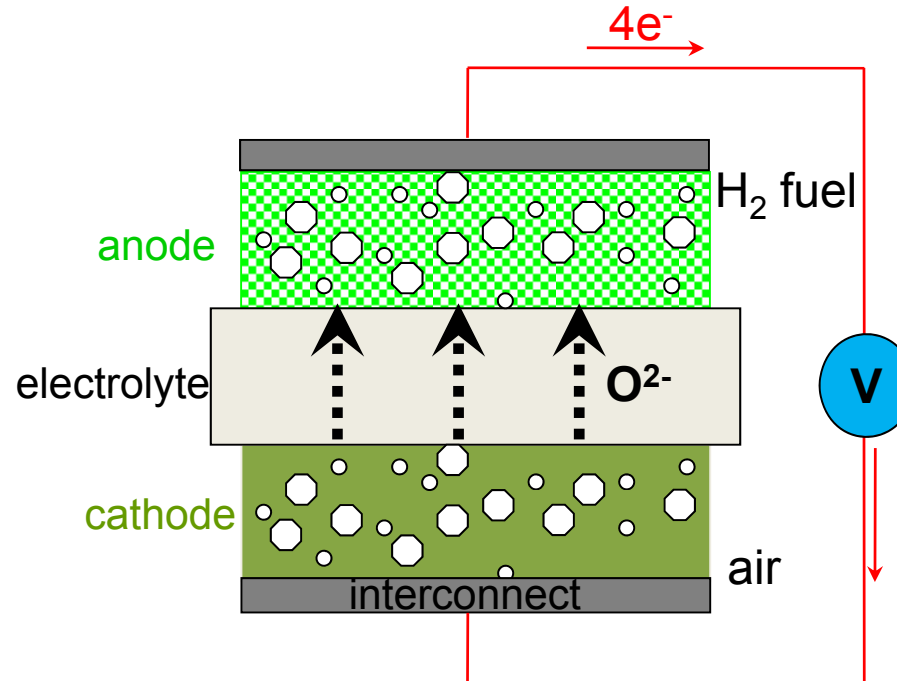
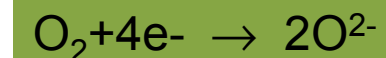
Overall reaction:



$$EMF(V) = \frac{RT}{4F} \ln \frac{P_{\text{O}_{2(\text{cat})}}}{P_{\text{O}_{2(\text{an})}}}$$

R Gas constant

F Faraday constant



**Cr-alloy interconnect
between cells of an
SOFC stack**

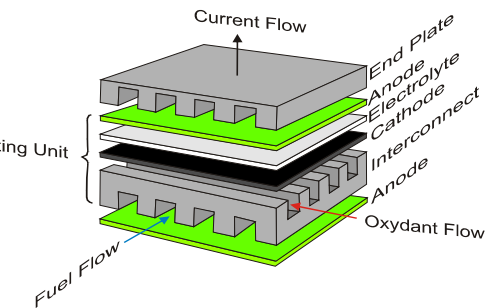
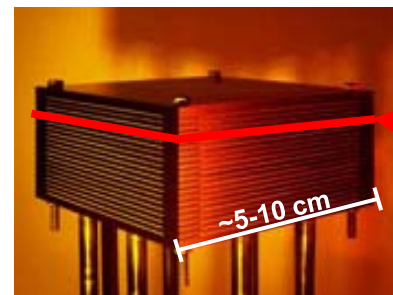
*Operating temperature:
800–1000 °C*

Direct conversion of chemical energy into electrical energy

High efficiency of energy conversion

From stack to system

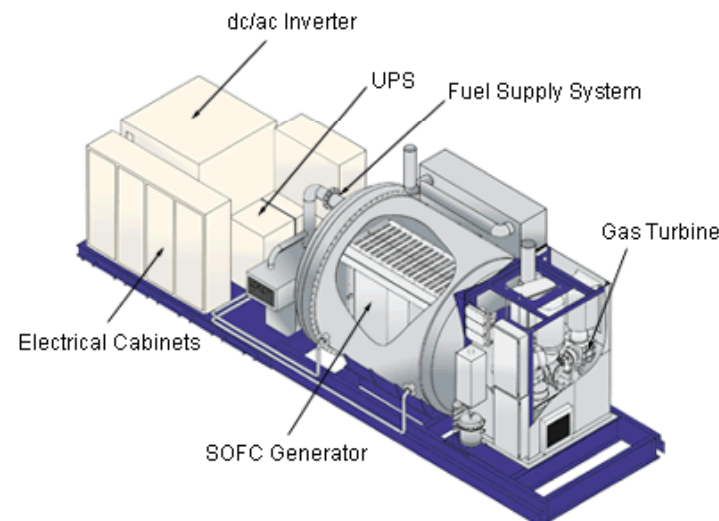
20 cells-stack



20 kW systems, 4000 h
to 10000 h

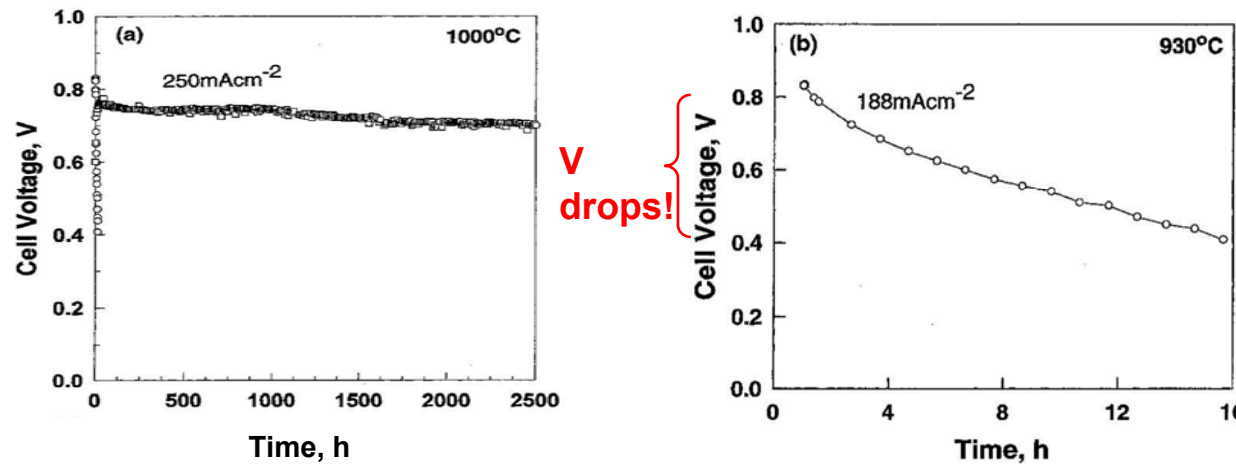


Future aim:
> 100 kW power plants
> 100000 h



Aim: high performance SOFC with **long-time stability** in the power plant scale

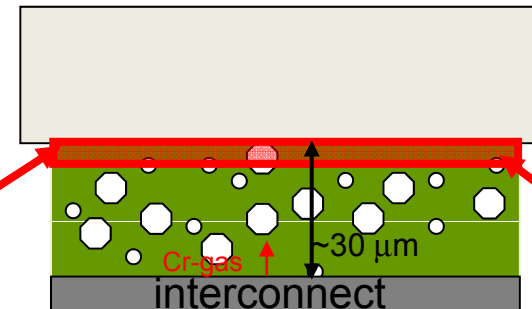
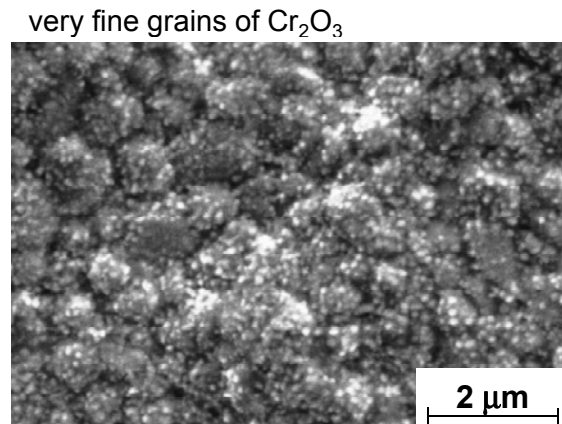
Degradation



LSM with Pt current collector
Degradation: 0.00001 V/hr

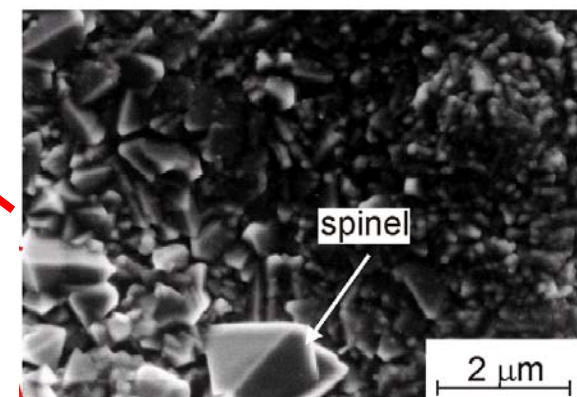
LSM with 94Cr5Fe1Y₂O₃ interconnect
Degradation: 0.025 V/hr

S.P.S. Badwal et al.: Solid State Ionics, 1997, 99, 297.



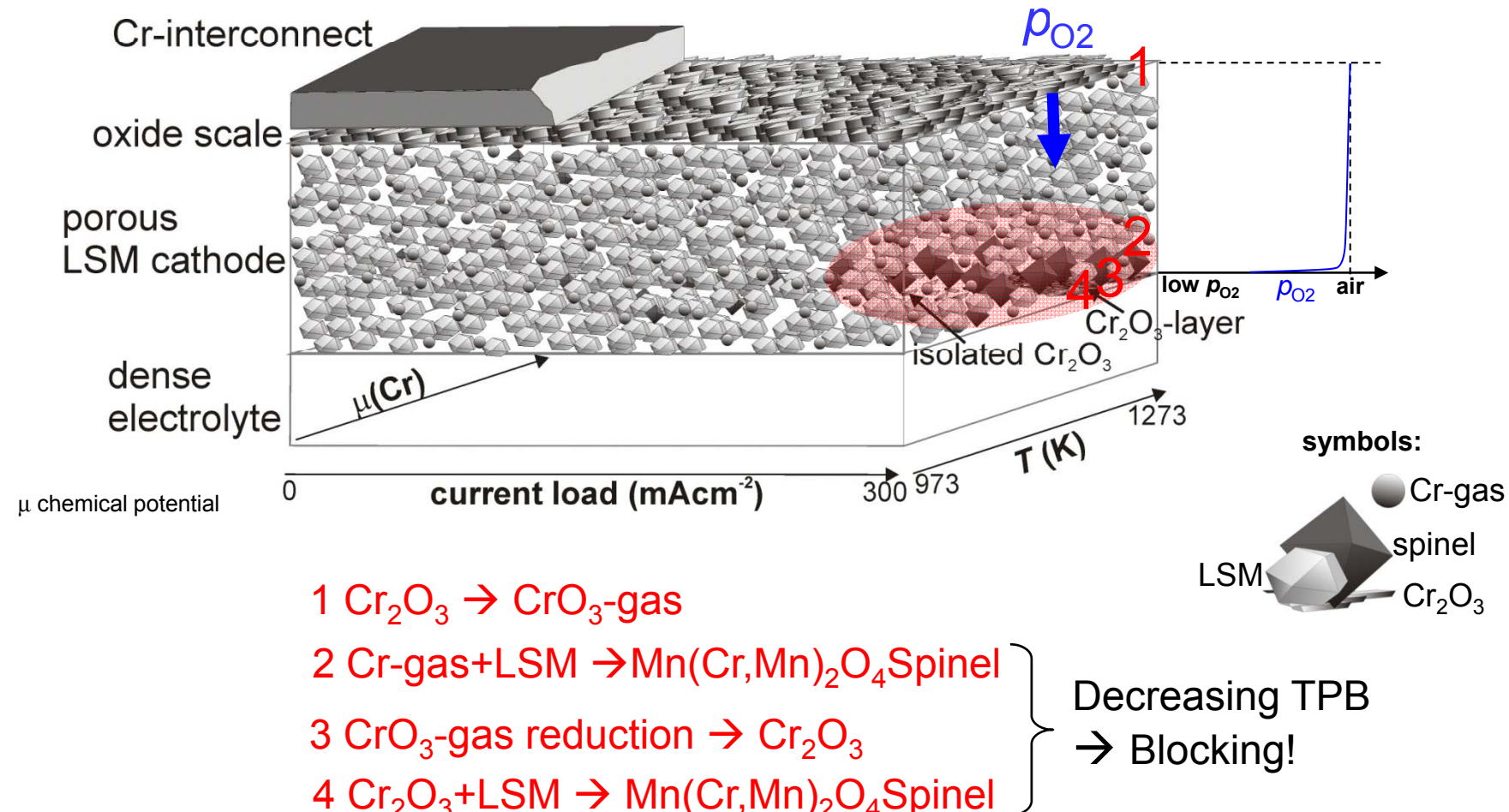
Observed Cr-deposits:
Mn(Cr,Mn)₂O₄ spinel, Cr₂O₃

SEM images from:
Jiang, S.P. et al.:
J. Electrochem. Soc. 148(7), 2001. C 477-55.



SOFC degradation is caused by **chromium from the interconnect**

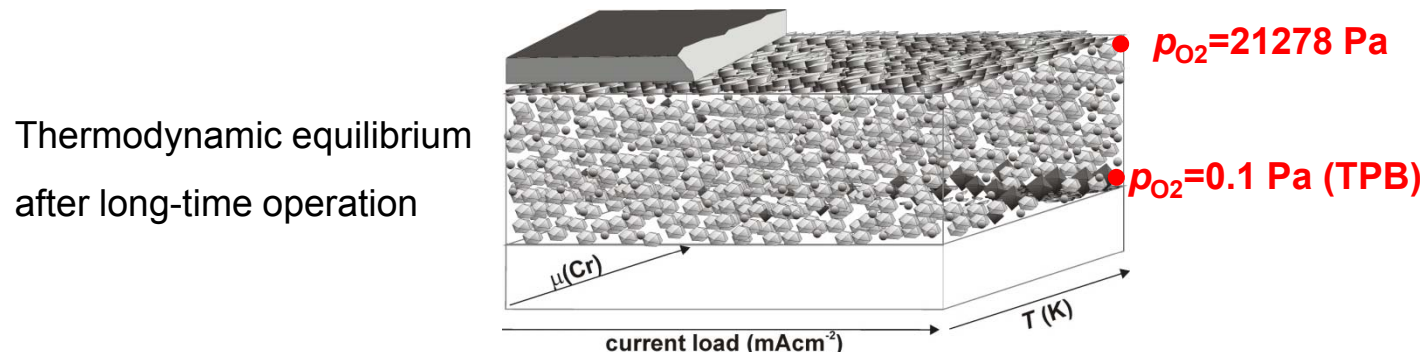
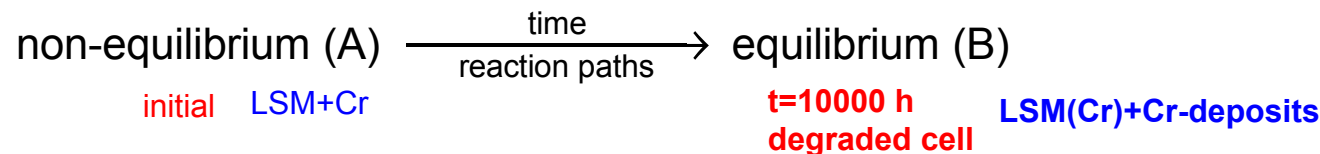
Mechanisms and microstructures



TPB = triple phase boundary LSM/YSZ/ $\text{O}_{2(g)}$, place of oxygen reduction.
New phases block pores.

Open questions

-) Thermodynamics → concentration of deposits at the cathode-electrolyte interface?
-) Thermodynamics → Cr compounds + LSM → ? → properties?
-) Reaction mechanisms to $\text{Mn}(\text{Cr},\text{Mn})_2\text{O}_4$ spinel?

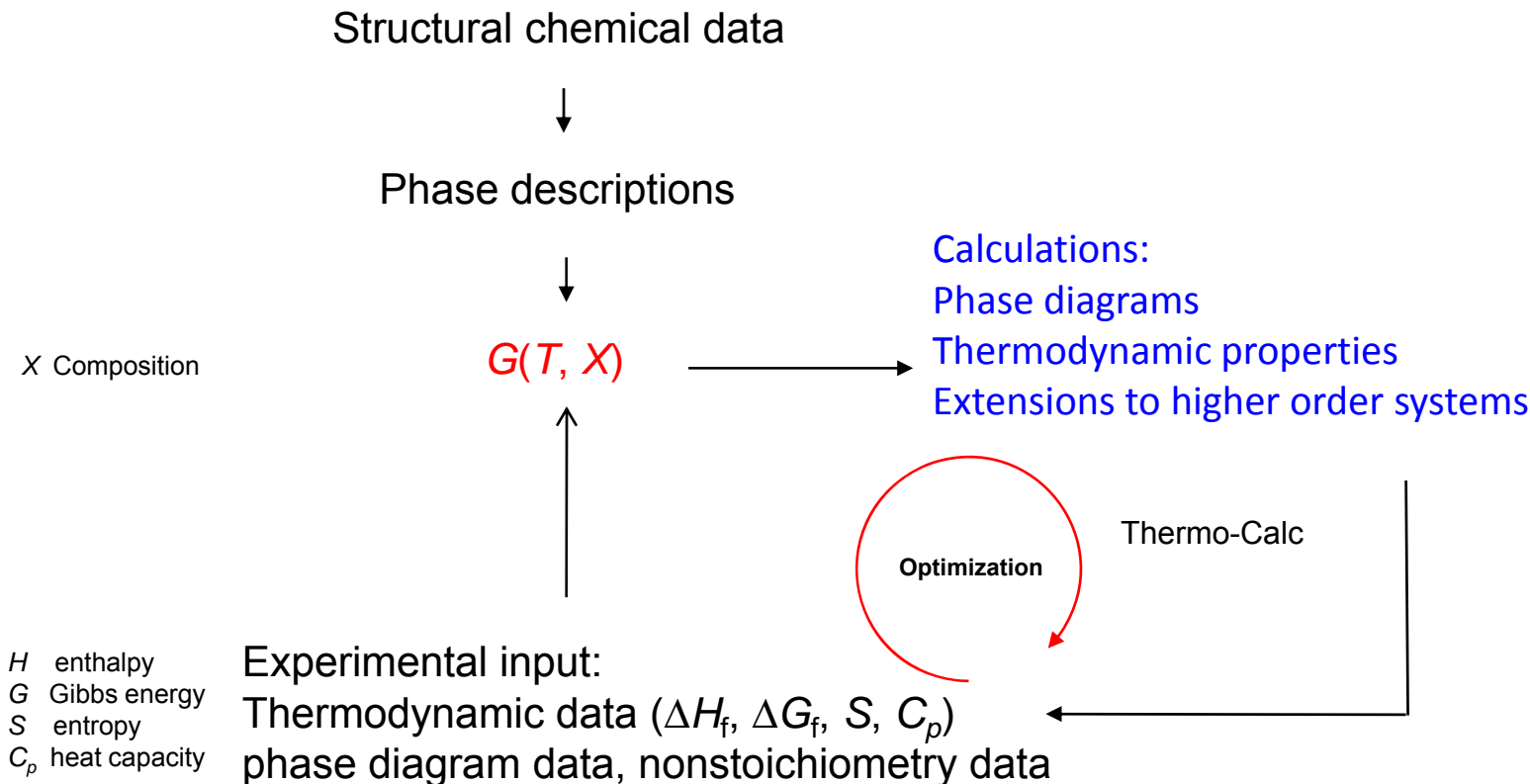


→ LSMCrO → Calculations of local thermodynamic equilibria in degraded SOFC

The construction of a thermodynamic database is a fundament for **future kinetic modeling**.

CALPHAD Modeling

Calphad (=Calculation of Phase Diagrams) modeling



Stoichiometric phase

$G(T)$ at $p, X=\text{constant}$

$$\Delta^\circ G = A + BT + CT \ln T + DT^2 + ET^3 + FT^{-1}$$

$$\Delta G = \Delta H - T\Delta S$$

$$\Delta S = -\left(\frac{\partial G}{\partial T}\right) = -B - C(1 + \ln T) - 2DT - 3ET^2 + FT^{-2}$$

$$\Delta H = \Delta G + T\Delta S = A - CT - DT^2 - 2ET^3 + 2FT^{-1}$$

$$C_p = \left(\frac{\partial H}{\partial T}\right) = -C - 2DT - 6ET^2 - 2FT^{-2}$$

Thermodynamic properties can be derived from the Gibbs energy polynomial

Example: stoichiometric Cr_2O_3

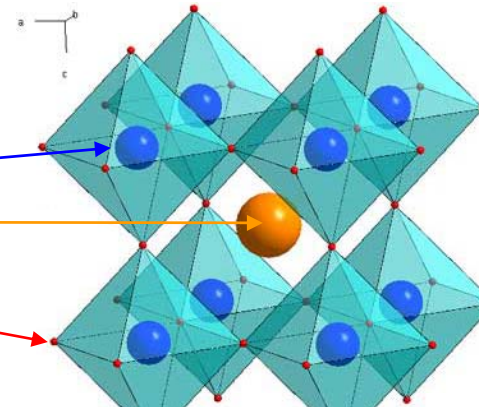
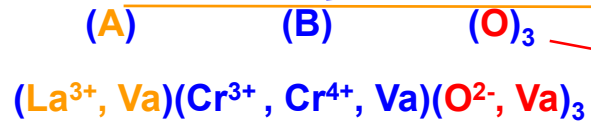
$$\Delta G_{\text{Cr}_2\text{O}_3} = -1164542 + 728.56T - 119.8T \ln T - 4.97 \times 10^{-3}T^2 + 1050000T^{-1}$$

The Gibbs energy function of a stoichiometric phase is achieved by **fitting model parameters (A to F)** to experimental thermodynamic and phase diagram data

Nonstoichiometric solid solution phases: Perovskite $\text{La}_{1-x}\text{Cr}_{1-y}\text{O}_{3-\delta}$

$G(T,X)$ at $p=\text{constant}$

General sublattice model



Stoichiometric endmember:
 $(\text{La}^{3+})(\text{Cr}^{3+})(\text{O}^{2-})_3$

$$G^{\text{prv}} =$$

Gibbs energy of endmember compounds

$$\sum_i \sum_j \sum_k y_i y_j y_k {}^\circ G_{i:j:k}$$

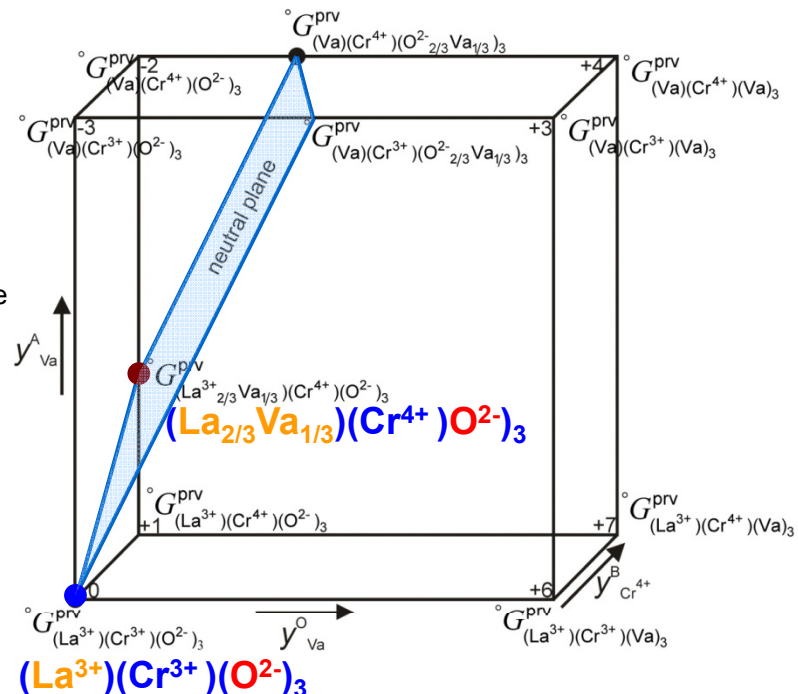
y site fraction
fraction of a species in a sublattice

Configurational entropy of ideal mixing

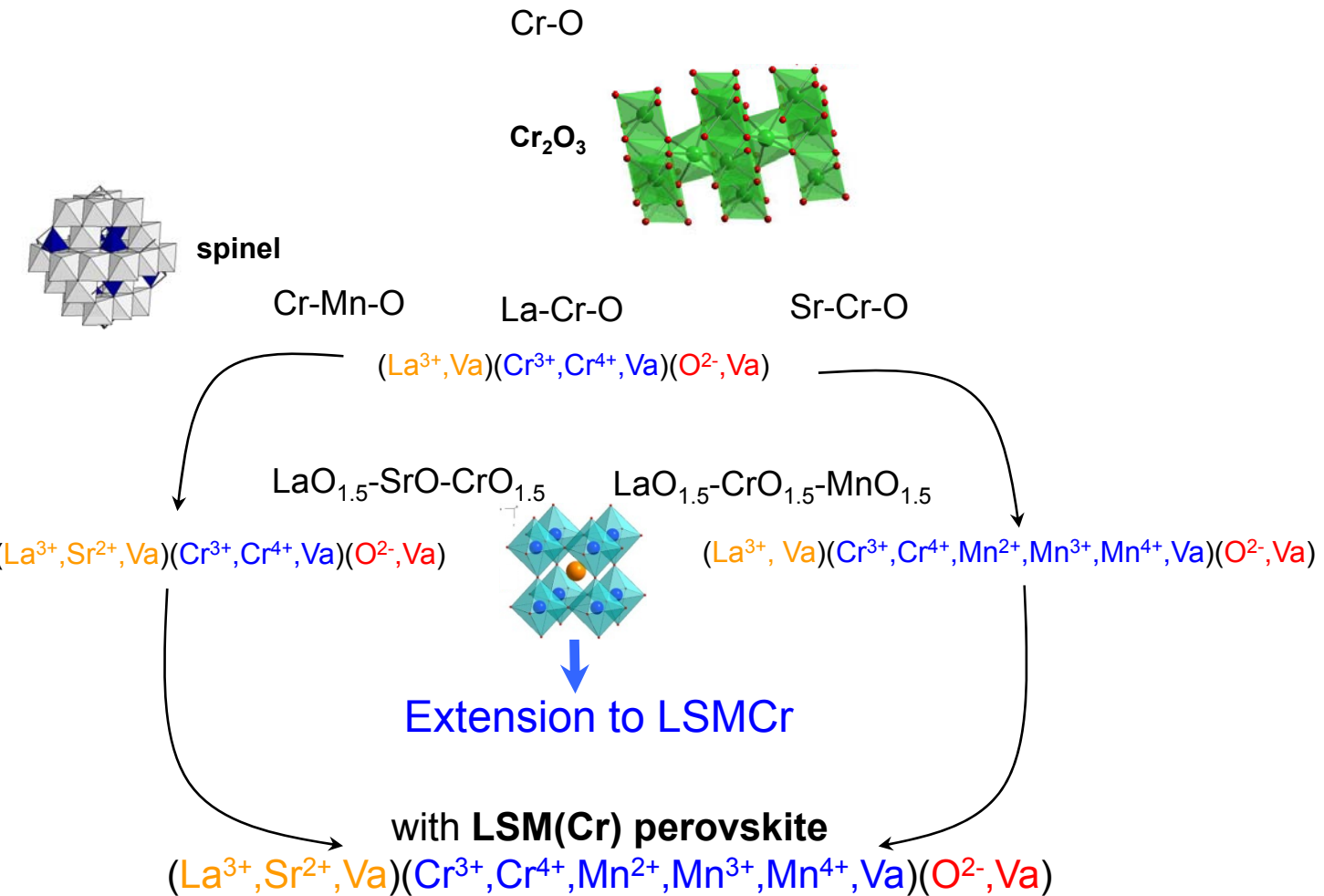
$$+RT \left(\sum_i y_i \ln y_i + \sum_j y_j \ln y_j + \sum_k y_k \ln y_k \right)$$

Excess Gibbs energy due to interactions

$$+ {}^E G^{\text{prv}}$$



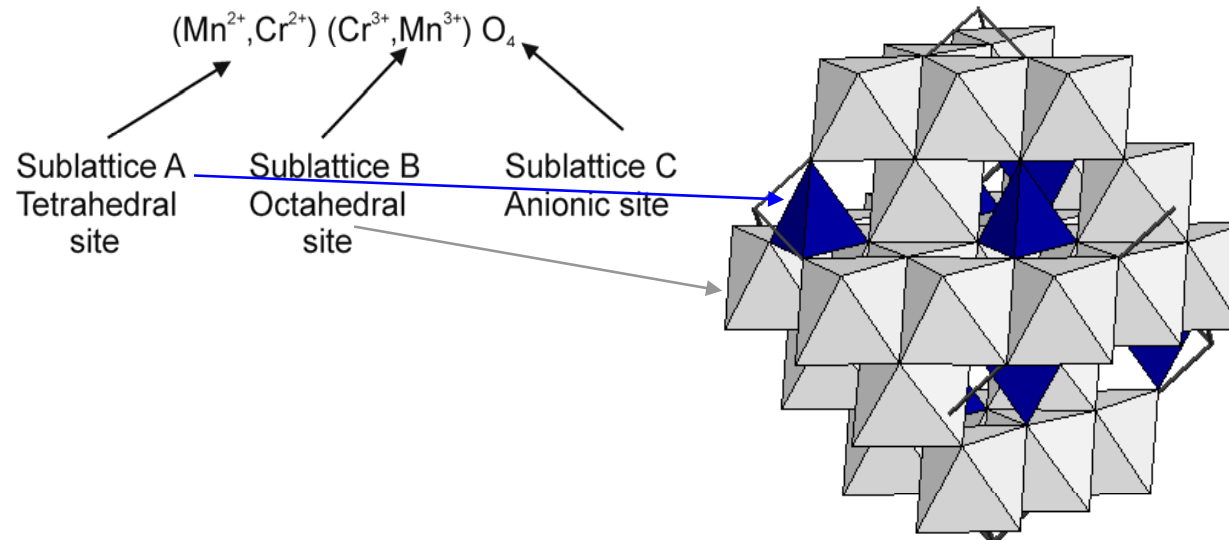
Assessed subsystems



Strategy: Optimize low-order subsystems first, then extend modeling to higher orders.

Extension from pseudoquaternaries to LSMCr without additional model parameters

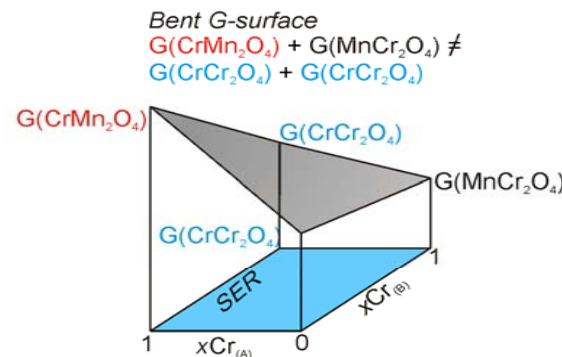
Cr-Mn Spinel



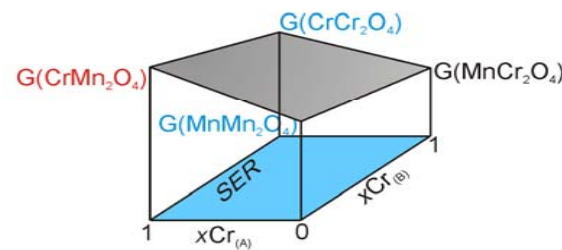
Compounds in cubic Mn-Cr-spinel
 $(\text{Mn}^{2+},\text{Cr}^{2+})(\text{Cr}^{3+},\text{Mn}^{3+})_2\text{O}_4$:



➤ Gibbs energies for each compound is defined

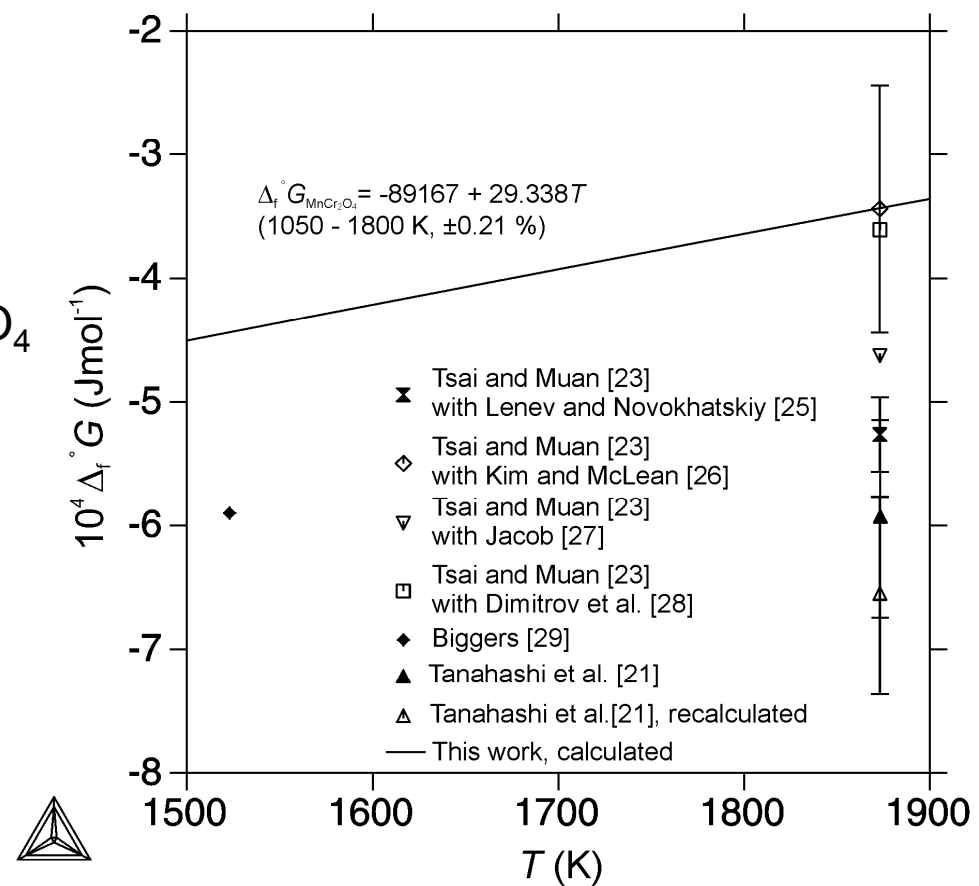


Flat G-surface

$$G(\text{CrMn}_2\text{O}_4) + G(\text{MnCr}_2\text{O}_4) = G(\text{CrCr}_2\text{O}_4) + G(\text{CrCr}_2\text{O}_4)$$


Thermodynamic data

Standard Gibbs energy of formation
of cubic spinel of the composition MnCr_2O_4



MnO_x-CrO_{1.5} phase diagram

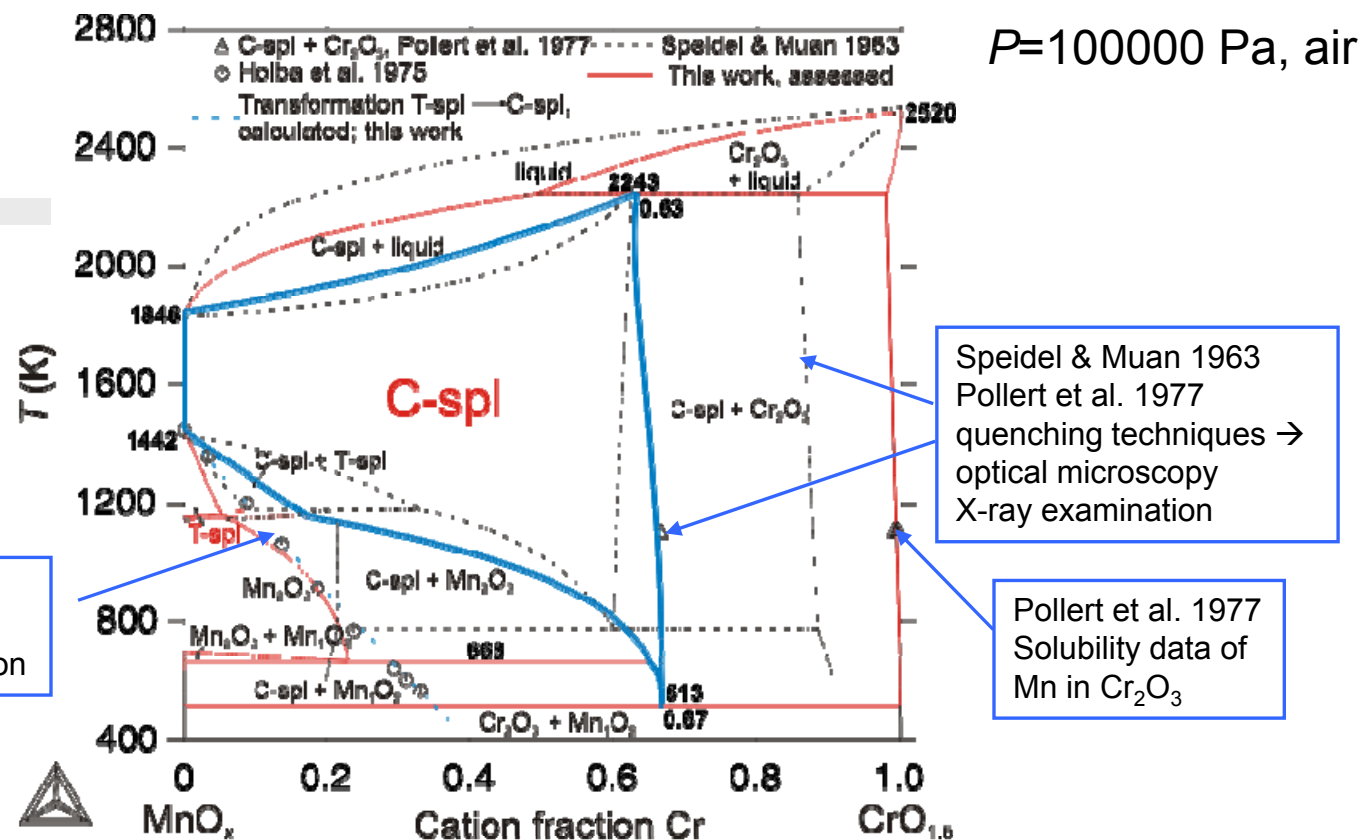
Cubic spinel (C-spl)



diffusionless phase transition

Tetragonally distorted
spinel (T-spl)
 $(\text{Mn})[\text{Cr,Mn}]_2\text{O}_4$

Holba et al. 1975
data of diffusionless
T-spl → C-spl transition



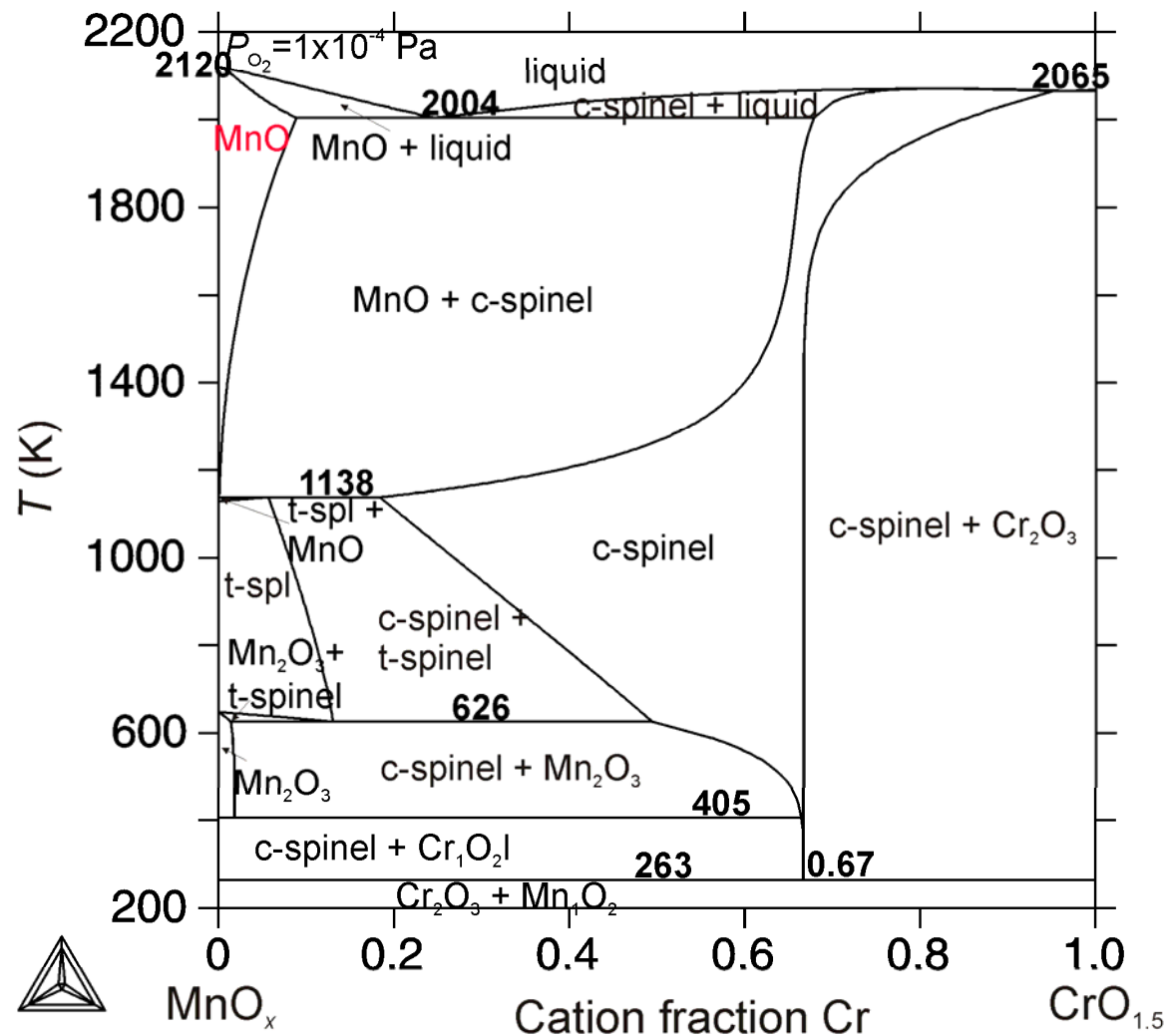
Povoden et al., Int. J. Mat. Res., 97(5), 2006

Cubic spinel is the dominating phase in air in a wide temperature range

Tetragonally distorted spinel is stable at the Mn-rich side of the section

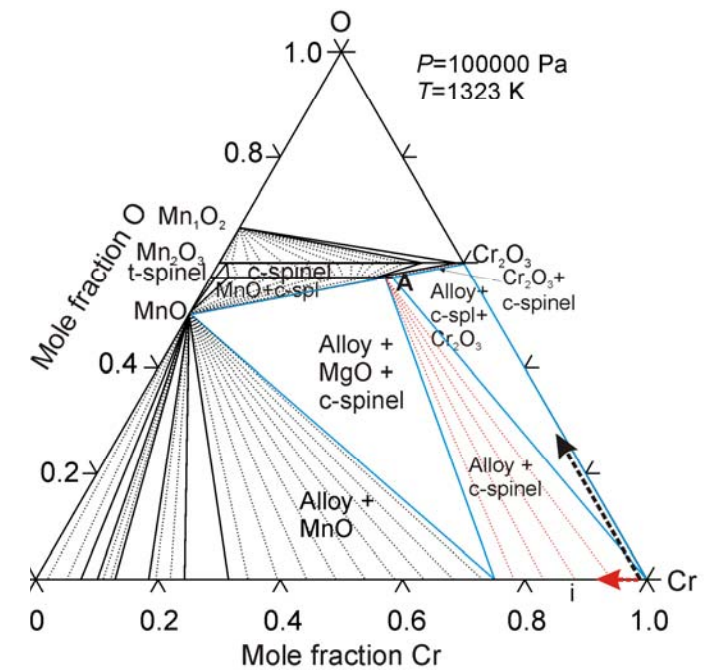
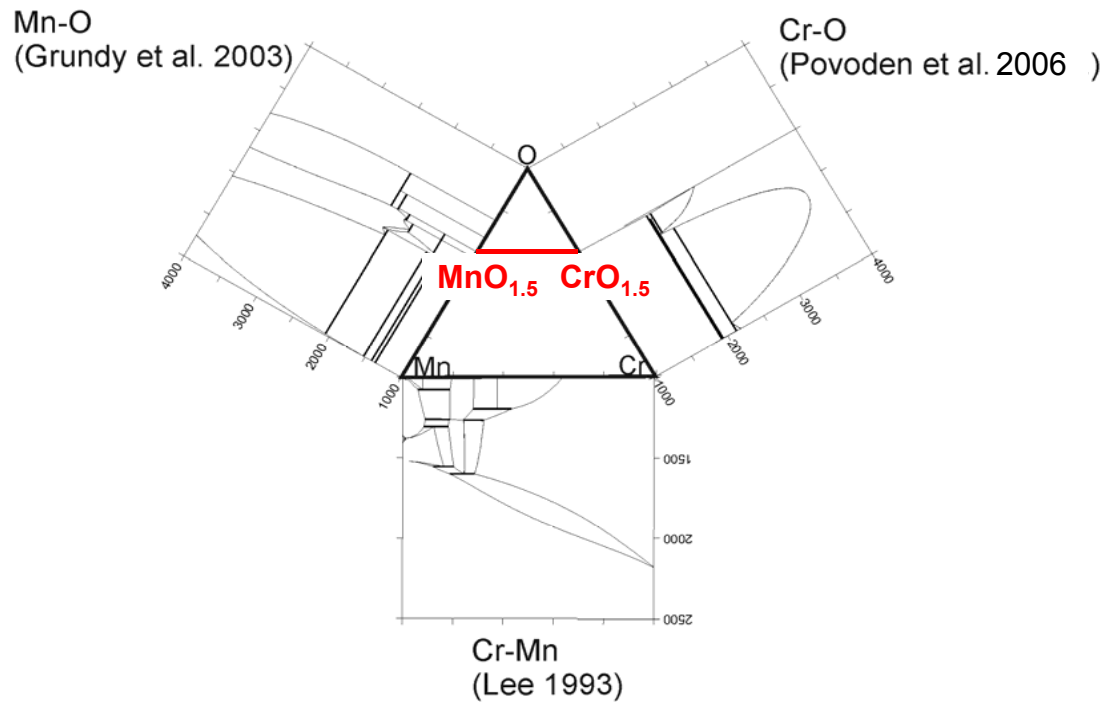
Good fit of the model description with data from Pollert et al. and Holba et al.

Calculation under low oxygen partial pressures



Ternary phase diagram

Mn-Cr-O



Perovskite

La-Cr-O oxide subsystem



Enthalpy of formation from oxides

This work:

$$\Delta_f H^\circ = -73700 \text{ J mol}^{-1}$$

Literature:

$$\checkmark \Delta_f H^\circ = -77163.5 \text{ J mol}^{-1}$$

Cheng & Navrotsky 2005



Good agreement

Standard entropy

This work:

$$S^\circ = 109.2 \text{ J K}^{-1} \text{mol}^{-1}$$

Literature:

$$\checkmark S^\circ = 111 \text{ J K}^{-1} \text{mol}^{-1}$$

Vishnyakow and Suponitskii 1985

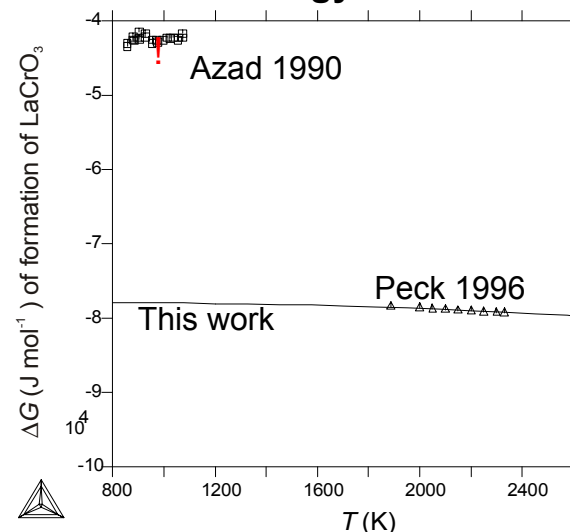
$$\checkmark S^\circ = 114 \text{ J K}^{-1} \text{mol}^{-1}$$

Yokokawa et al. 1991, est.

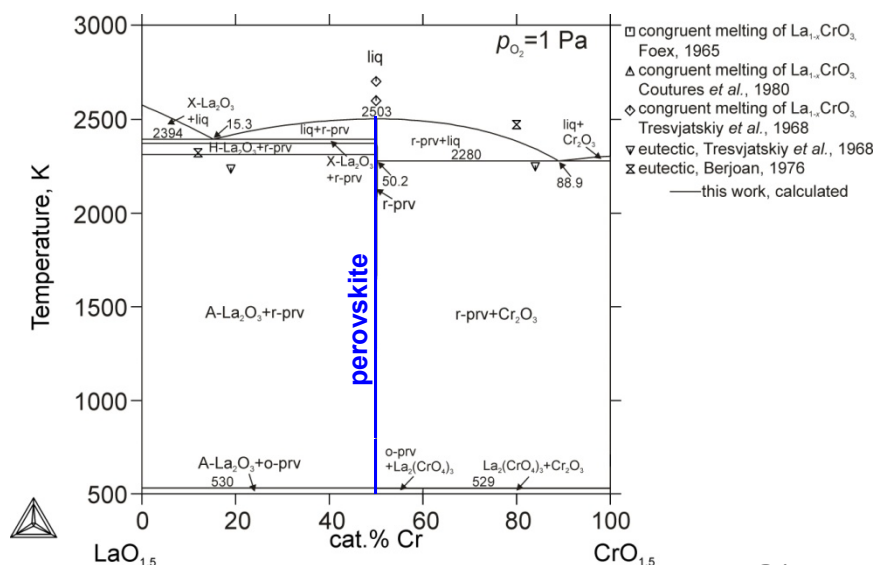
$$S^\circ = 87 \text{ J K}^{-1} \text{mol}^{-1}$$

Azad et al. 1990

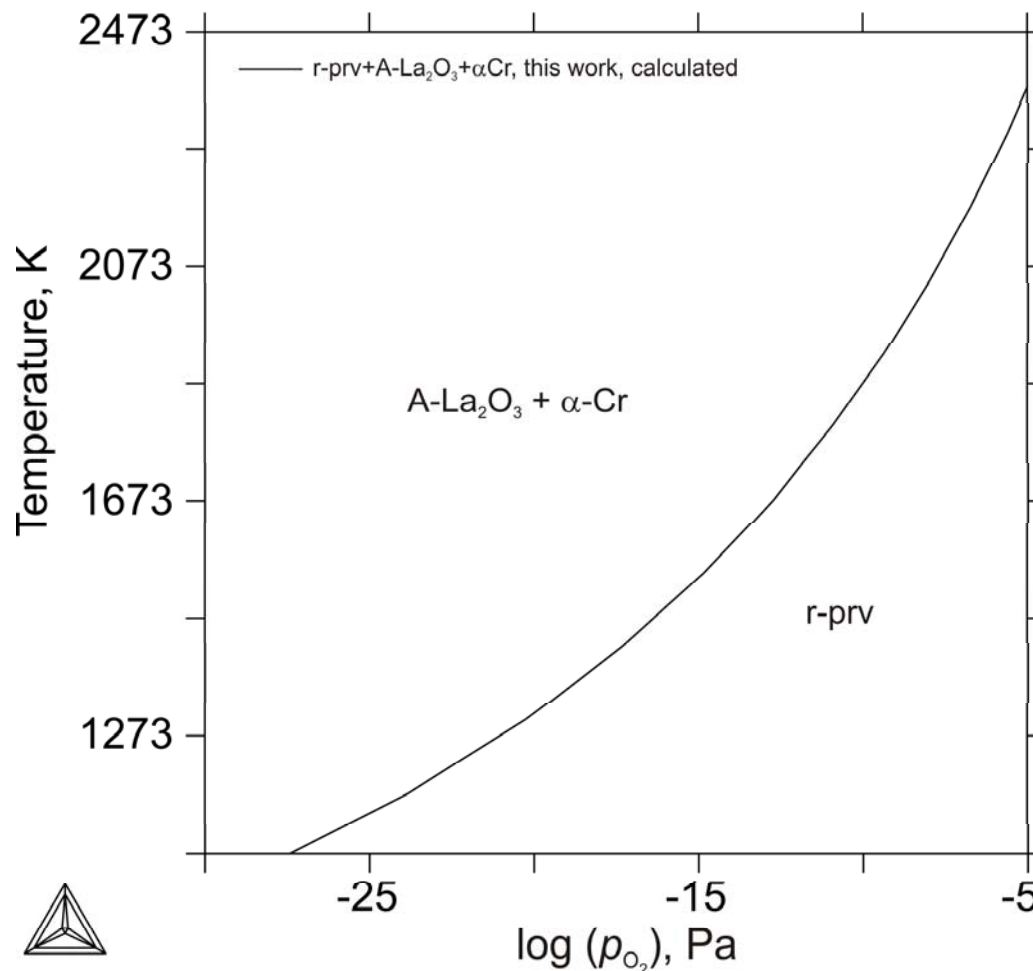
Gibbs energy of formation



Experimental phase diagram data
→ decision for the correct set of thermodynamic data



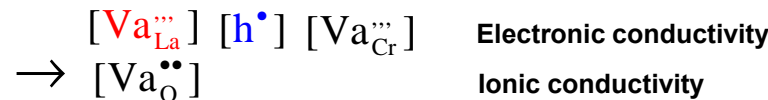
Calculated stability of rhombohedral La-Cr-perovskite



Defect concentrations of nonstoichiometric La-Cr perovskite



Defect chemistry can be modeled!



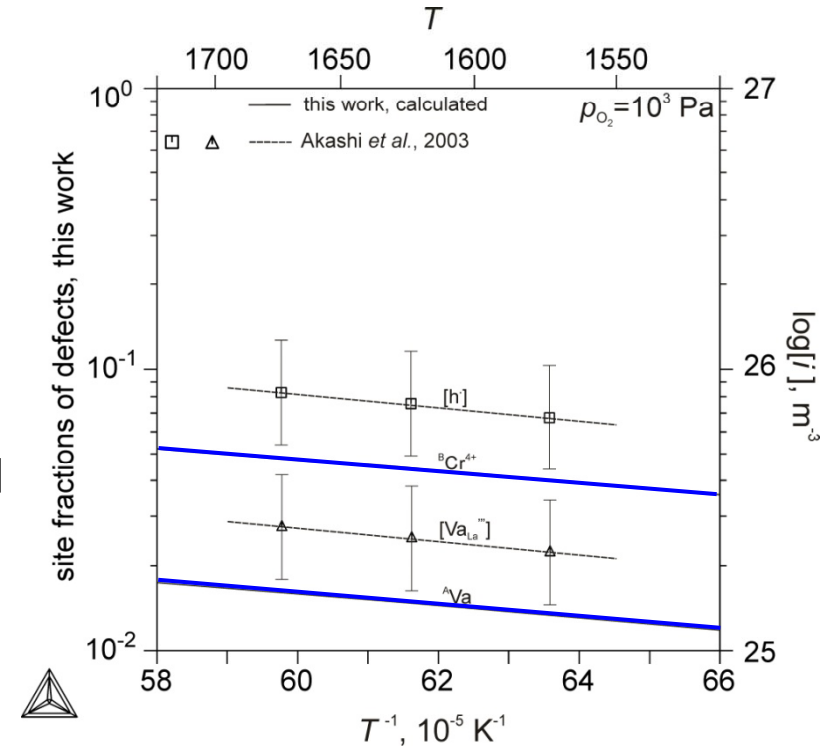
as a function of T and p_{O_2}

$$\sigma_{\text{LaCrO}_3} = e\mu_{\text{Va}_{\text{La}}^{\cdot\cdot\cdot}} [\text{Va}_{\text{La}}^{\cdot\cdot\cdot}] + e\mu_{\text{Va}_{\text{Cr}}^{\cdot\cdot\cdot}} [\text{Va}_{\text{Cr}}^{\cdot\cdot\cdot}] e\mu_\text{h} [\text{h}^\bullet] + e\mu_{\text{Va}_\text{O}^{\bullet\bullet}} [\text{Va}_\text{O}^{\bullet\bullet}]$$

σ electrical conductivity
 μ defect mobility
 e elementary charge



Predictions on electronic and ionic conductivities



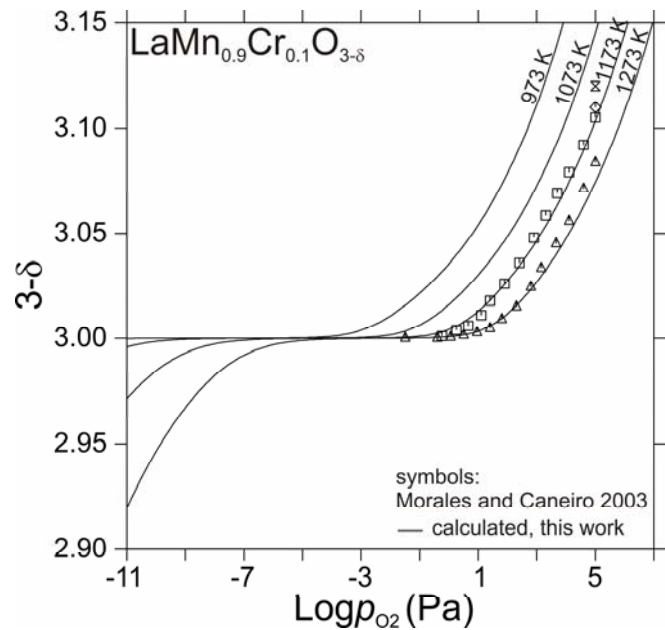
Advantage of modeling defect chemistry with Calphad:

Thermodynamically consistent (Gibbs energies of compounds)

Straight-forward extension to high-order systems

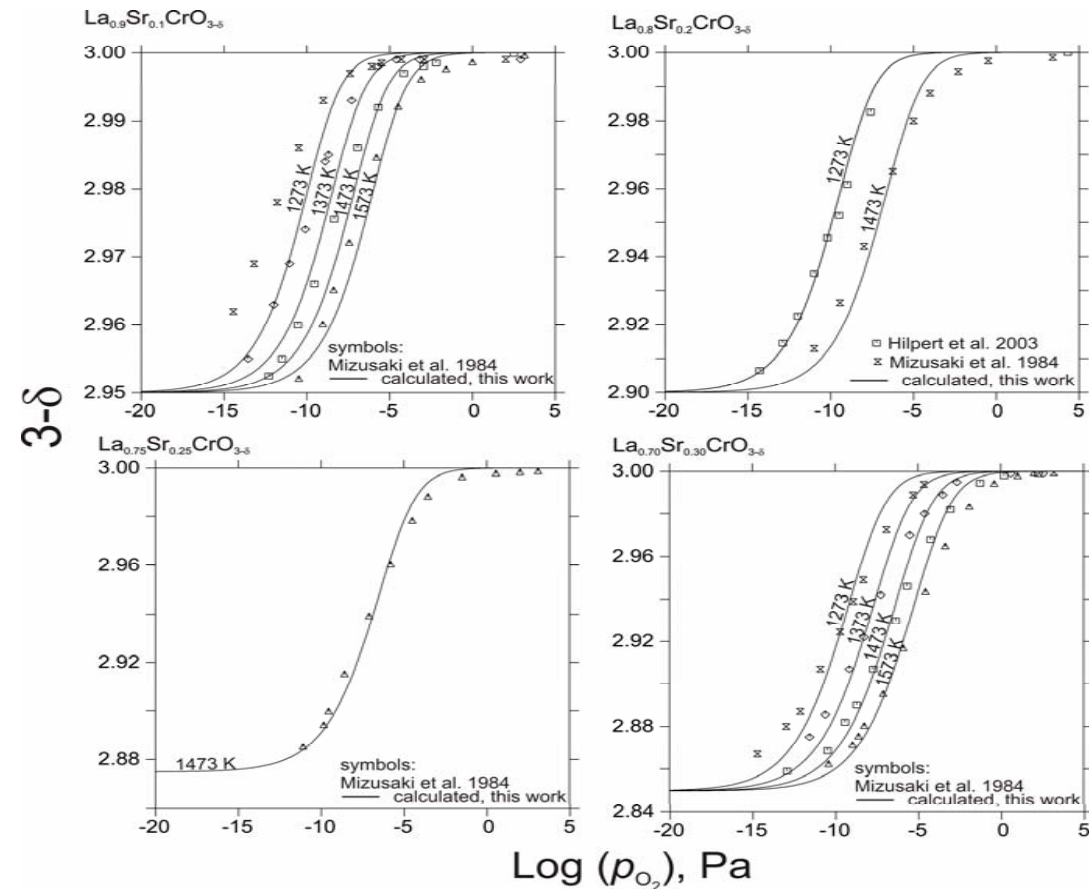
Oxygen nonstoichiometry in $\text{La}_{1-x}\text{Mn}_x\text{CrO}_{3-\delta}$ perovskite

$(\text{La}^{3+}, \text{Va})(\text{Cr}^{3+}, \text{Cr}^{4+}, \text{Mn}^{2+}, \text{Mn}^{3+}, \text{Mn}^{4+}, \text{Va})(\text{O}^{2-}, \text{Va})$



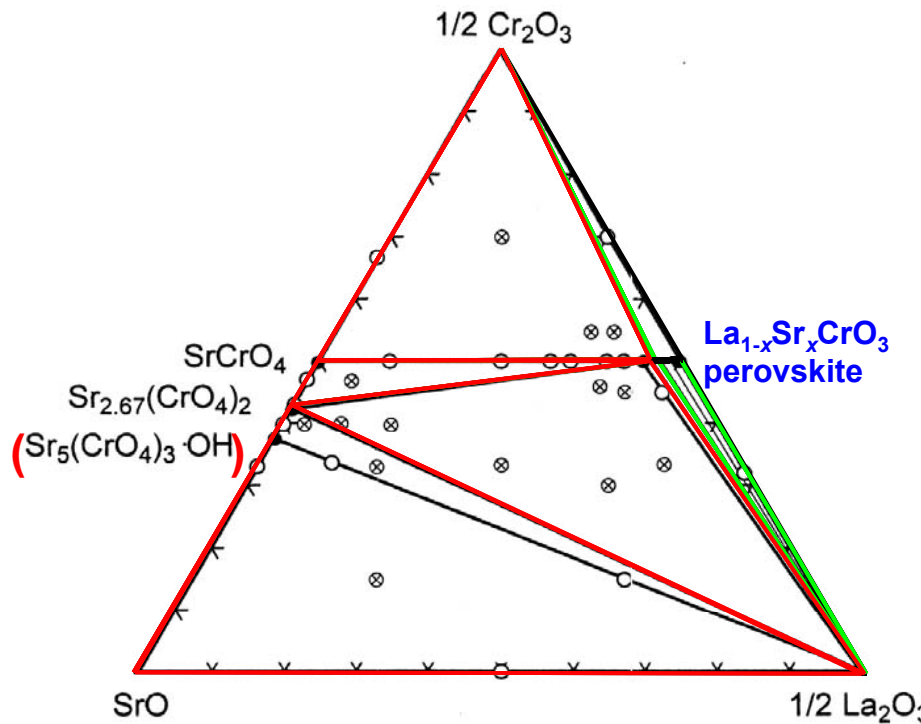
Oxygen nonstoichiometry in $\text{La}_{1-x}\text{Sr}_x\text{CrO}_{3-\delta}$ perovskite

$(\text{La}^{3+}, \text{Sr}^{2+}, \text{Va})(\text{Cr}^{3+}, \text{Cr}^{4+}, \text{Va})(\text{O}^{2-}, \text{Va})$



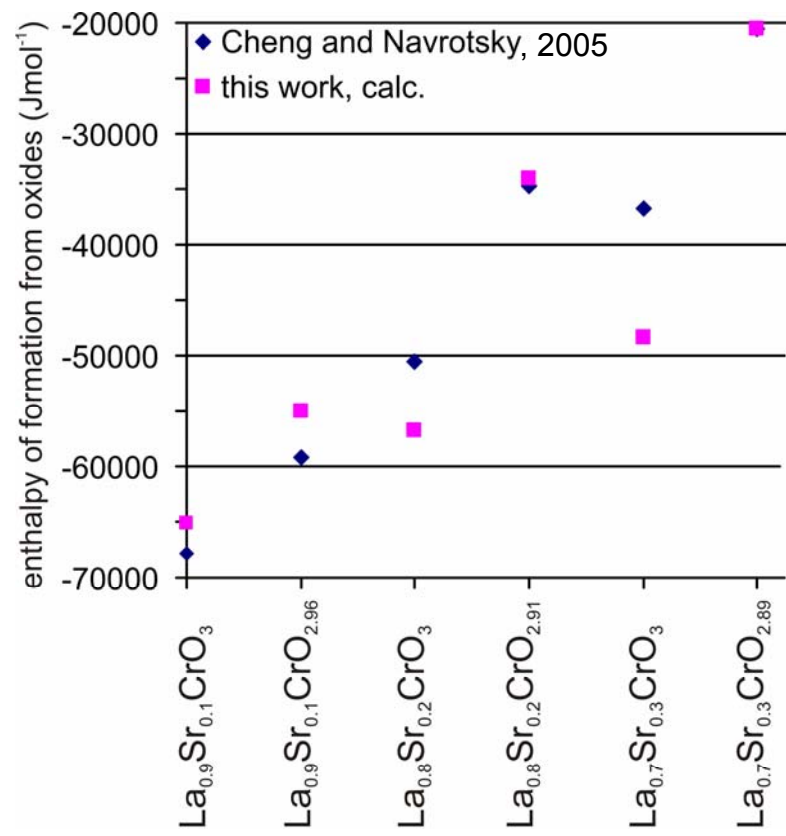
La-Sr-Cr-O oxide subsystem

$\text{LaO}_{1.5}$ – SrO – $\text{CrO}_{1.5}$ air, 1223 K



D.H. Peck et al., Solid State
Ionics 123, 1999, 59-65.

$\text{La}_{1-x}\text{Sr}_x\text{CrO}_{3-\delta}$ perovskite
enthalpy of formation from oxides at 298 K



Summary of results in assessed oxide subsystems

✓ Thermodynamic properties are well reproduced
✓ Phase diagrams are reproduced by the modeling
✓ Defect chemistry is well reproduced by the model

Applications: Equilibrium calculations of SOFC cathodes poisoned by chromium

→ Extension without additional parameters to the higher order system:
 La-Sr-Cr-Mn-O

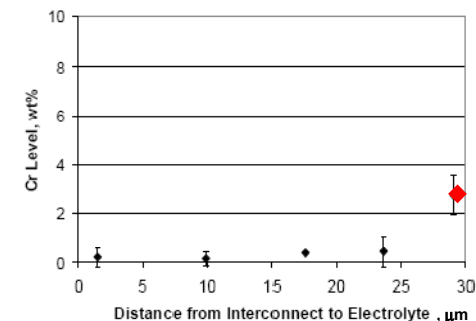
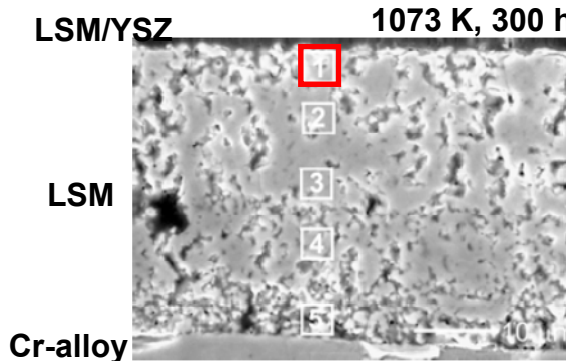
Cr-gas+LSM → Spinel

Composition of cathode: $(La_{0.8}Sr_{0.2})_{0.9}MnO_3$

Conditions: Operation temperature: 1073 – 1273 K

Where to get the appropriate chemical potential of chromium?

- 1.) from Cr content at the cathode/electrolyte interface of degraded cell:
Cr level \approx 3 wt%



Krumpelt et al., FY Annual report, 2004, 39-43.

- 2.) from oxygen partial pressure:**

assumption: oxygen vacancies exist in LSM at triple phase boundary (TPB)

A. Hammouche et al., J. Electrochem. Soc., 1991, 138, 1212.

T. Horita et al., J. Electrochem. Soc., 2001, 148, J25-30.

G.J. la O' et al., J. Electrochem. Soc., 2007, 154, B427-B438.

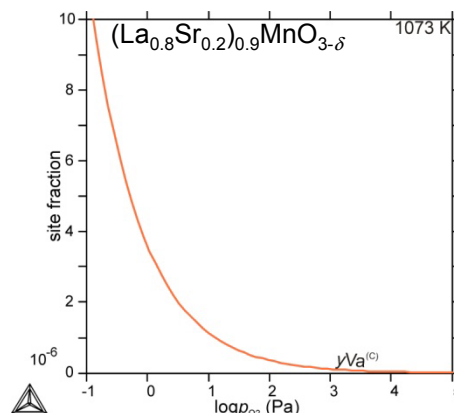
Calculation: from polarisation

→ $p_{O_2} > 0.1 \text{ Pa}$ at TPB

→ Chemical potential of chromium

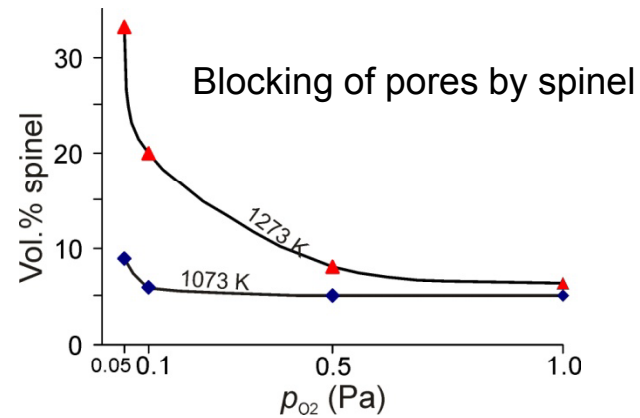
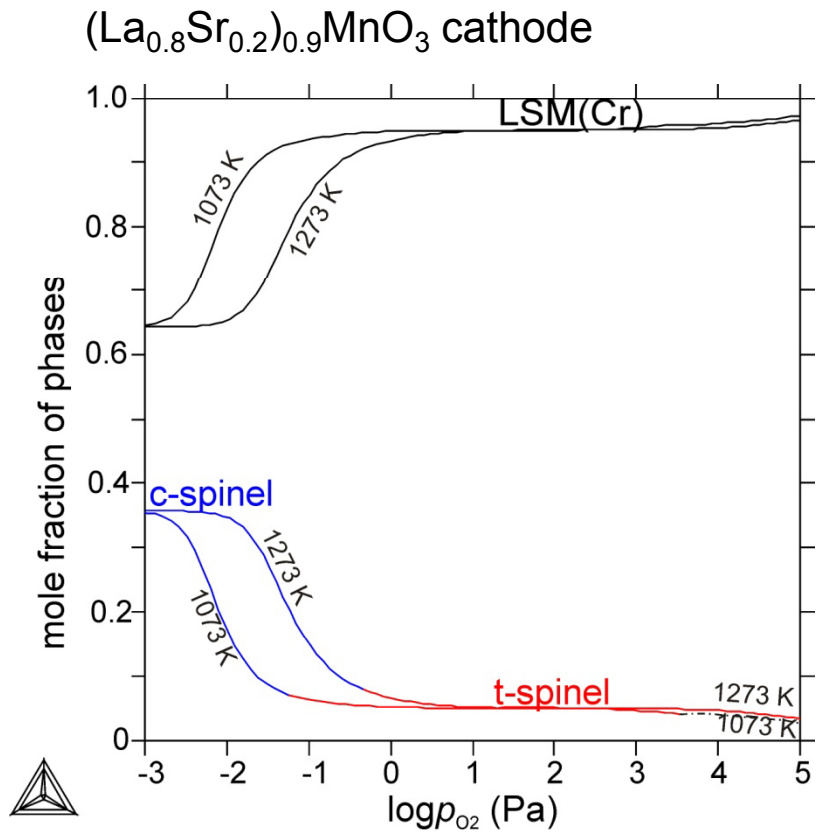
$$\mu \approx -300 \text{ kJmol}^{-1}$$

Reference: 10^5 Pa CrO_{3(q)}

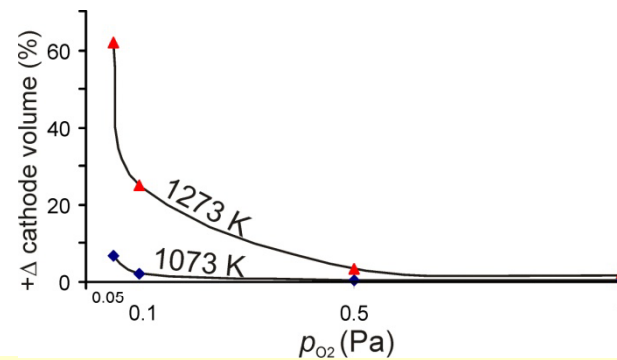


A.N. Grundy et al.,
Calphad 28, 2004, 191-201

Equilibria in degraded SOFC



Density data used:
 Cr-Mn spinel: $\rho = 4.85 \text{ gcm}^{-3}$ (Kubaschewsky and Hopkin 1967)
 LSM: $\rho = 6.557 \text{ gcm}^{-3}$ (Pelosato et al. 2005)



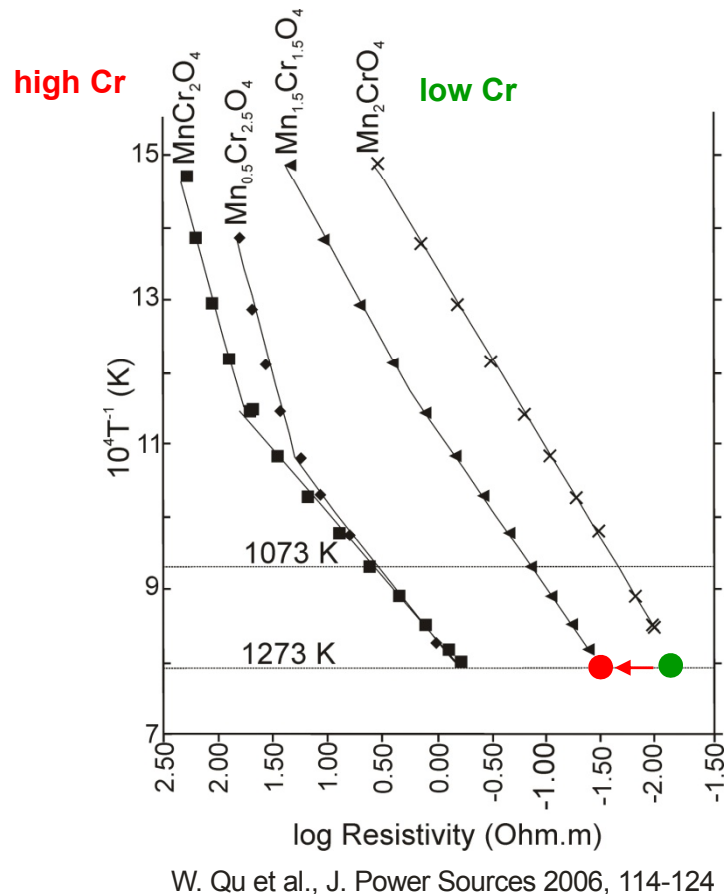
Cubic spinel forms at low p_{O_2} in Cr-poisoned LSM.

At lower temperatures c-spinel formation is shifted towards lower p_{O_2} .

No Cr₂O_{3(s)} is found in thermodynamic equilibrium.

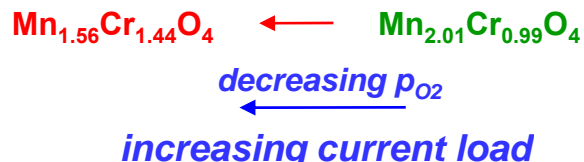
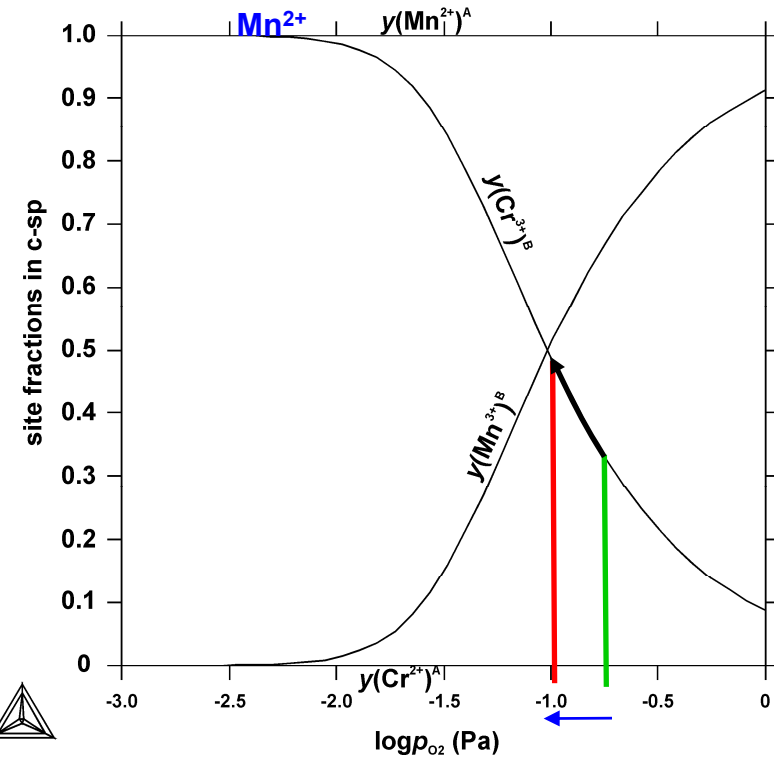
Spinel tends to **clogg pores** at high T and low p_{O_2} .

Composition of spinel and electrical conductivity



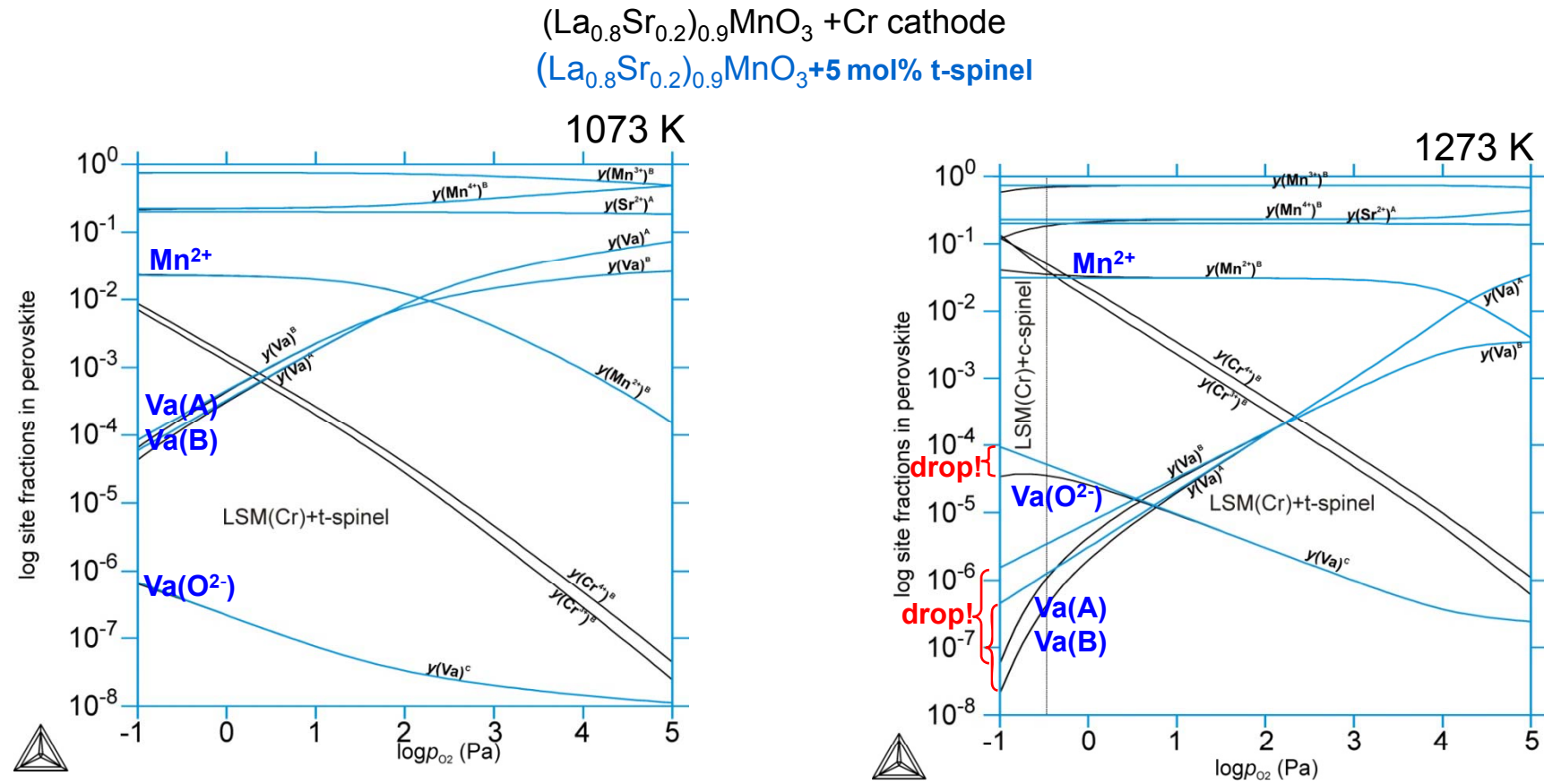
$(La_{0.8}Sr_{0.2})_{0.9}MnO_3$ cathode

$(La_{0.8}Sr_{0.2})_{0.9}MnO_3 + c\text{-sp}$
 $P=100000 \text{ Pa}, T=1273 \text{ K}$
 $\mu(CrO_3)=-300000 \text{ J mol}^{-1}$, ref.: $100000 \text{ Pa } CrO_{3(g)}$,



Low p_{O_2} : More chromium in spinel \rightarrow lower electrical conductivity

Defect chemistry of cathode



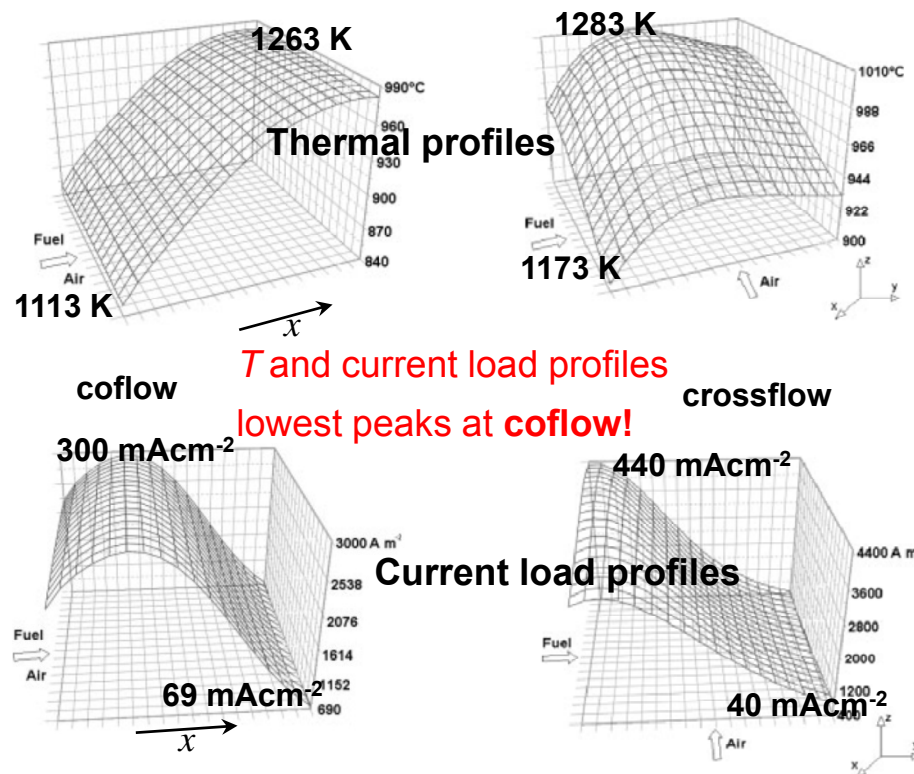
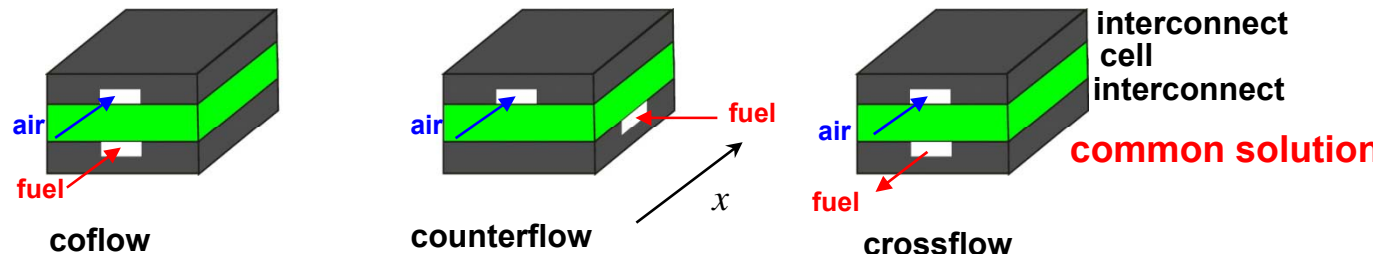
Considerably lower defect concentrations in LSM(Cr) than in LSM at $p_{\text{O}_2} < 1 \text{ Pa}$ at high $T \rightarrow$ lower electrical conductivity of LSM(Cr)

High Mn²⁺ at $p_{\text{O}_2} < 3500 \text{ Pa}$ at high $T \rightarrow$ favors spinel formation

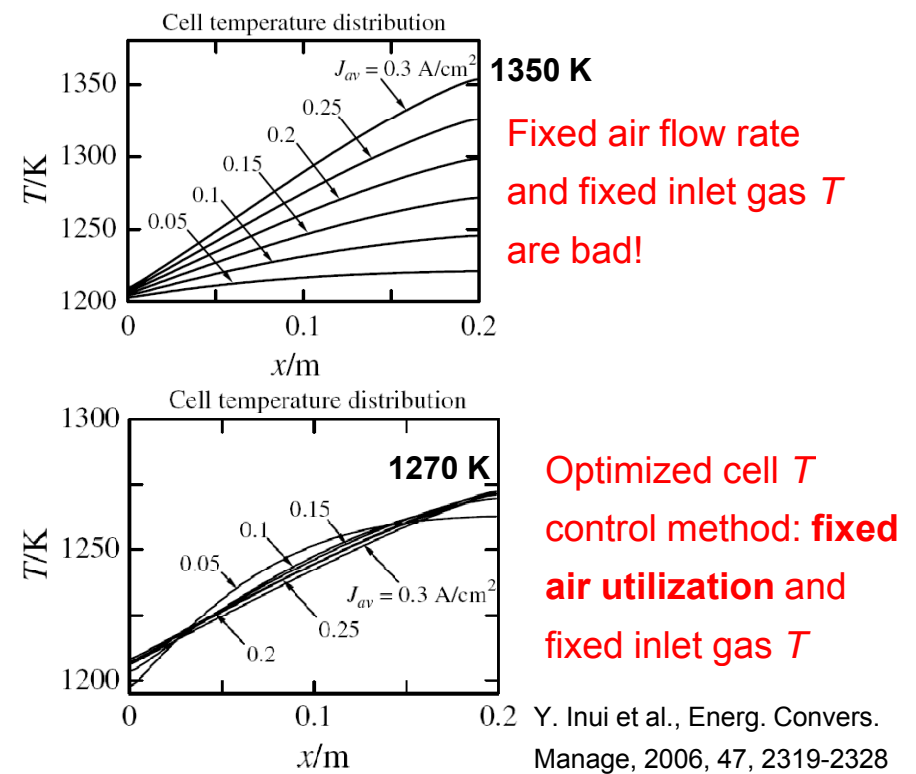
Conclusions

- $(A,Va)(B,Va)(O^{2-},Va)_3$ perovskite model from low to high order systems.
- Thermodynamics → LSM(Cr)+spinel, no Cr_2O_3
- Thermodynamics → High T , low p_{O_2}
 - Spinel blocks pores at TPB
 - High Mn^{2+} in LSM(Cr), thus favored $(Mn^{2+})(Cr^{3+},Mn^{3+})O_4$ spinel formation
 - more chromium in spinel and changing defect concentrations, hence decreasing electrical conductivity.
- **Thermodynamics → Lower operation T and lower current load (thermodynamically: higher p_{O_2}) means less degradation**

Outlook – Multiscale modeling



S. Campanari and P. Iora, Fuel Cells, 2005, 5, 34-51

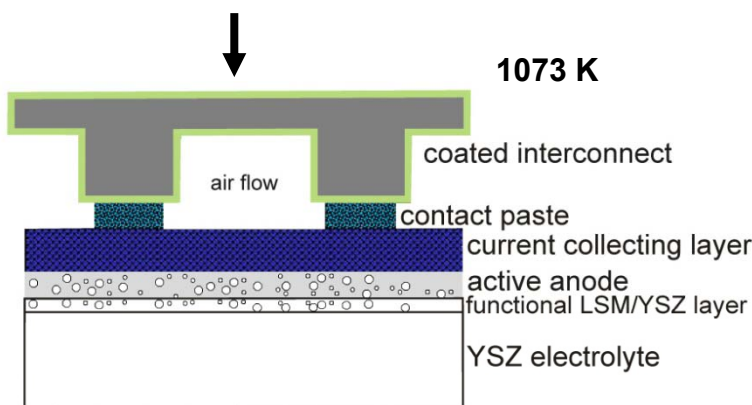


Y. Inui et al., Energ. Convers. Manage, 2006, 47, 2319-2328

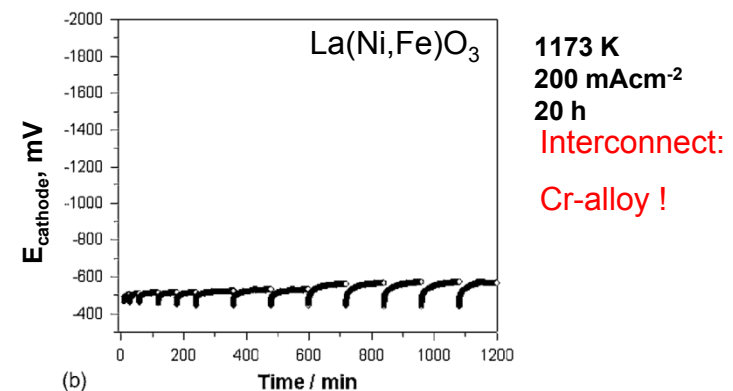
Conventional materials – Optimization

& New ways – alternative materials

- Improvements for calculations:
quantitative p_{Cr}
 - Cr \longleftrightarrow YSZ interactions
Cr + LSM-YSZ functional layers
 - La-Sr-Mn-Cr-Y-Zr-O
oxide database
 - LSM \longleftrightarrow coatings:
La-Sr-Mn-O-Cr-Co,
Co-Fe, Co-Ce, Cu, Ni



- Promising new cathode perovskites:
 $(La,Sr)(Co,Fe)O_3$ ✓ La-Sr-Fe-O
 $(Ba,Sr)(Co,Fe)O_3$
 - Highly chromium-tolerant cathodes:
 $La(Ni,Fe)O_3$ perovskite
 $(La,Ba)(Co,Fe)O_3$ perovskite



- LaCrO₃-based ceramic interconnects
 - La-Sr-Ca-Cr-O
 - La-Sr-Ca-V-Cr-O
 - La-Ca-Zn-Cr-O

Outlook – Kinetic modeling

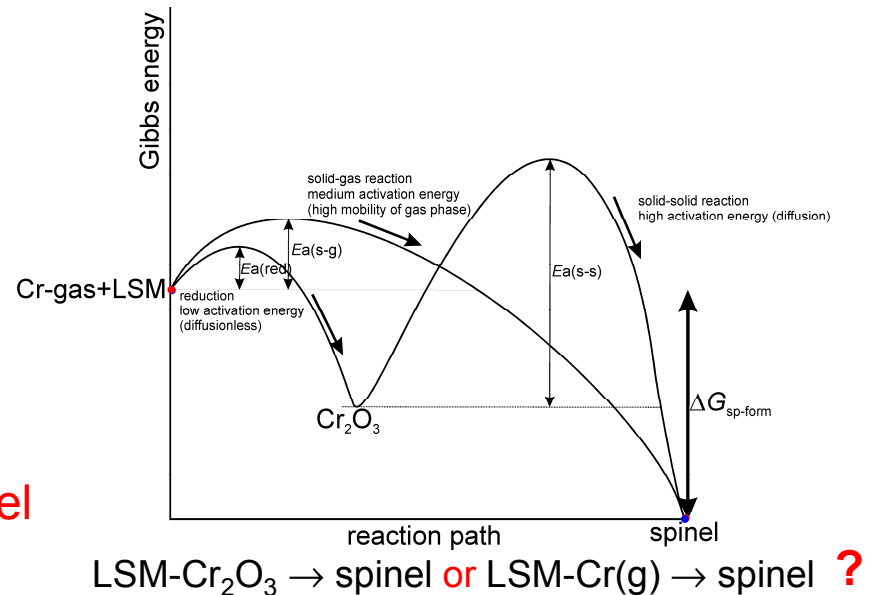
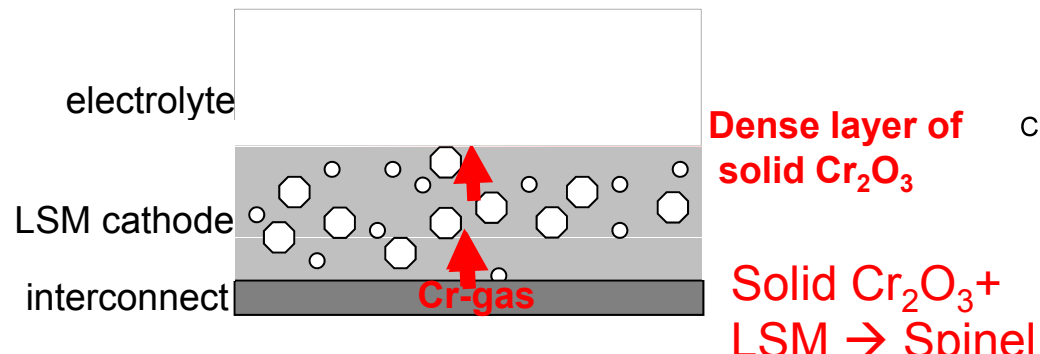
non-equilibrium $\xrightarrow{\text{time}}$ equilibrium ✓

surface mechanisms –
early stages of degradation:

Several ppm of Cr lead to significant decrease of oxygen diffusion

(J. Zheng and P. Wu, 4th international symposium on solid oxide fuel cells, and pers. comm.)

time, reaction rates



Thermodynamic LSMCr oxide database + algorithms and mobility databases → modeling of kinetics